Identification of therapeutic targets in coronary artery disease: from patient to mice and back

Kraaijeveld, A.O.

CHAPTER 10

Myocyte enhancer factor 2 activity disruption is detrimental for endothelial cell function and induces atherosclerotic plaque erosion

Adriaan O. Kraaijeveld
Markus Lucerna
Menno Hoekstra
Ralph J. van Oort
Saskia C.A. de Jager
Theo J.C. van Berkel
J. Wouter Jukema
Leon J. de Windt
Erik A.L. Biessen

Manuscript submitted

ABSTRACT

Background: Recently, a MEF2A genetic deletion was identified that imparts an increased risk for coronary artery disease and myocardial infarction, suggesting a role of MEF2 family members in these disorders. This led us to investigate whether focal MEF2 activity modulation may affect plaque stability.

Methods and Results: MEF2 activity was modulated in pre-existing carotid artery plaques in Western type diet fed apoE-/- mice (N=21) by transluminal transduction with constitutively active MEF2 adenovirus (Ad-caMEF2), dominant negative MEF2 (Ad-dnMEF2) or Ad-empty. Two weeks post transduction, plaque size as well as cellular composition were unaffected by MEF2 activity modulation. However, severe plaque erosion was observed in Ad-dnMEF2 infected plaques, only as evidenced by diminished $CD31^+$ staining ($P<0.001$) which was accompanied by a high incidence of intraplaque haemorrhage in Ad-dnMEF2 versus sham treated groups (38 vs. 3% iron-positive plaques; $P<0.01$). In keeping, subcutaneous injection of Matrigel containing adenoviral vectors into C57/Bl6 mice revealed a clear inhibition of infiltrative cellular growth in Ad-dnMEF2 (N=5) compared to Ad-empty plugs. In vitro endothelial cell sprouting in Matrigel was markedly impaired after Ad-dnMEF2 versus Ad-empty infection, while conversely Ad-caMEF2 induced a pro-angiogenic effect. Microarray analysis revealed striking overlaps between MEF2 and VEGF signalling, while vital pathways were seen to be suppressed upon Ad-dnMEF2 infection. Conclusion: MEF2 is a potent mitogenic and proangiogenic transcription factor to vascular wall cells *in vitro* and *in vivo* partly through a VEGF-like effect. Of clinical relevance, disruption of MEF2 mediated transcription is accompanied by plaque erosion and intraplaque haemorrhage *in vivo*.

INTRODUCTION

In the last decade, major advances in genomic technology have led to the identification of several genes or genetic polymorphisms that predispose to or protect against cardiovascular disease [1]. Illustratively, genetic linkage analysis has revealed a 7 amino acid deletion in the MEF2A gene that is responsible for an autosomal dominant pattern of coronary artery disease within one single family [2]. This mutation dramatically reduced MEF2A transcriptional activity. MEF2A was found to be specifically expressed by endothelial cells of coronary arteries, but it is still unclear whether and how its expression pattern or function under pathological conditions can contribute to disease development.

The Myocyte Enhancer Factor 2 (MEF2) family of DNA-binding transcription factors consists of 4 isoforms, MEF2A, -B, -C and –D. Although it has been extensively studied in the context of vertebrate (heart) muscle development, its expression by various vascular wall cell constituents points to a role in the regulation of calcium signaling pathways and thereby influences vascular homeostasis [3]. Inhibition of MEF2A function has been shown to aggravate neointimal formation in wire-injured mouse femoral arteries [4]. Furthermore, MEF2A-/- mice were non-viable, while heterozygotes exhibited a seemingly normal phenotype. These findings suggest that almost complete knock-down of MEF2A might be required to promote CAD [5]. In line with this finding, MEF2C deficient mice were not capable of forming a normal heart and vascular system [6]. Importantly, MEF2A and MEF2C are the predominant isoforms expressed in vascular cells [3]. MEF2A was undetectable in contractile vascular smooth muscle cells (VSMCs), whereas MEF2A expression was induced in proliferative VSMCs, suggesting a role for MEF2A in the regulation of VSMC behaviour in CAD [7]. Furthermore, MEF2C function is crucial for proper endothelial cell metabolism, however its downstream target genes remain to be identified [8,9].

Collectively, these findings suggest a potential role for MEF2 in vascular homeostasis and cardiovascular disease, but a direct causal contribution of MEF2 to CAD remains to be established. Hereto, we assessed the effects of adenoviral MEF2 silencing or overexpression in advanced atherosclerotic plaques on plaque homeostasis and stability. We show that perturbation of MEF2 activity leads to diminished endothelial cell function culminating in plaque erosion and intraplaque haemorrhage, both features of enhanced plaque vulnerability, and, by microarray, identify down-stream target genes and genetic pathways which influence MEF2 dependent endothelial cell function.

METHODS

Animals

Female ApoE deficient C57Bl6-J mice (N=21), aged 10-12 weeks, were obtained from our own breeding stock. Mice were placed on a Western-type diet containing 0.25% cholesterol and 15% cocoa butter (Special Diets Services, Witham, UK). High fat diet and water were provided

ad libitum. All animal work was approved by the regulatory authority of Leiden University and performed in compliance with the Dutch government guidelines.

Recombinant Adenoviruses

MEF2VP16, a fusion between amino acids (aa) 1-91 of human MEF2D and aa 412-490 of the viral transcriptional activator VP16, was cloned into the pAdTrack-CMV viral shuttle vector (provided by Bert Vogelstein, Johns Hopkins University) and recombined in BJ5183 bacteria (Stratagene) to obtain E1-E3-deleted adenoviral bicistronic vectors to generate AdMEF2VP16, which expresses a constitutively active form of MEF2 (Ad-caMEF2) and Green Fluorescent Protein (GFP) under separate CMV promoters. Adenoviral vectors carrying a dominant negative form of MEF2 (Ad-dnMEF2) was generated as described previously [10]. Ad-empty-GFP (Ad-empty) was generated as described previously and used as a control vector [11]. All viral vectors tested negative for replication competent adenovirus as judged by PCR using GGGTGGAGTTTGTGACGTG as forward and TCGTGAAGGGTAGGTGGTTC as reverse primers.

Carotid Collar Placement and Transgene Expression

Carotid atherosclerotic lesions were induced by collar placement 2 weeks after starting Western-type diet as previously described [12]. Briefly, a constricting silastic collar (Dow Corning, Midland, MI) was placed on both carotid arteries inducing atherosclerotic lesion formation proximal to the collar within 4 weeks. The collars were thereafter removed and the plaque containing right carotid arteries were incubated intraluminally with 20 µl of an adenovirus suspension at a non-inflammatory titer of 1.5×10^{10} pfu/ml for ten minutes [13], whereas the left carotid arteries were sham operated. Vectors carried caMEF2 (Ad-caMEF2), dnMEF2 (Ad-dnMEF2) or an empty transgene (Ad-empty). The virus load was equalized in all groups to exclude cytotoxicity and related pro-inflammatory effects. Two weeks after local incubation, the mice were sacrificed and the carotids were prepared for histochemical analysis.

Tissue harvesting

Mice were sacrificed six weeks after collar placement. Before harvesting, the arterial bed was flushed for ten minutes with phosphate buffered saline (PBS) and formaldehyde (Formalfix, Thermo Shandon). Fixated carotid arteries were embedded in OCT compound (Sakura Finetek, Zoeterwoude, the Netherlands), snap frozen in liquid nitrogen and stored at -20°C until transverse, serial cryosections were prepared (5µm thick) on a Leica cryostat.

Staining procedures and plaque analysis

Carotid artery sections, stained with Hematoxylin (Sigma-Aldrich, Zwijndrecht, the Netherlands) and Eosin (Merck Diagnostica, Darmstadt, Germany), were used for morphometric analysis. Next to assessing GFP presence within plaques after quenching auto-fluorescence with Chicago Sky Blue, GFP was detected using a JL-8 antibody (Clontech, Mountain View, CA). Staining procedures for vascular smooth muscle cells (VSMCs), macrophages, collagen, iron presence as

well as endothelial CD31 were performed as previously described [14]. The relative area of $CD31^+$ plaque coverage of the total endothelial layer was measured. All histological analyses were performed on a Leica microscope with LeicaQwin analysis software (Leica Imaging Systems, Cambridge, UK).

Proliferation assay

Murine H5V endothelial cells were plated in 6-well plates, grown to 70% confluence in Dulbecco's Modified Eagle Medium (DMEM) supplemented with 10% fetal calf serum (FCS), 100 µg/ml streptomycin, 100U/ml penicillin and 2 mM L-glutamine, and transduced for three hours with Ad-caMEF2 and Ad-empty at 100 multiplicities of infection (MOI). After 18 hours of incubation on standard medium, cells were serum starved in DMEM + 0.5%. Cells were then incubated for 5 hours in standard medium containing 0.5 µCi [^{3}H]-thymidine (Amersham, Uppsala, Sweden). Thymidine incorporation was measured by a Packard 1500 liquid scintillation analyzer (PerkinElmer, Waltham, MA).

Matrigel sprouting assay

Human umbilical vein cells (HUVECs, $5x10^4$) were infected with Ad-caMEF2, Ad-dnMEF2 and Ad-empty (100 MOI) in Optimem + 0.5% FCS. After two days, cells were detached, resuspended in DMEM + 10% FCS, and subsequently $3x10^4$ cells were plated on Matrigel (BD Biosciences, San Jose, CA) coated 6-well plates. After 6 hours, pictures were taken of all the wells in a randomized manner and used for analyzing the number of cellular junctions, the length of connecting filopodia and the area of the picture covered by HUVECs using Leica Qwin analysis software.

Mouse Matrigel plug assay

In vivo angiogenesis was examined using wild type C57Bl6 mice, purchased from Charles River laboratories, which were subcutaneously injected in the groin area with 300 µl of Growth Factor Reduced Matrigel (BD Biosciences), mixed with $1x10^9$ pfu/ml of Ad-caMEF, Ad-dnMEF2 or Ad-empty (N=5 per group) with and without 200 ng/ml Vascular Endothelial Growth Factor (VEGF, R&D Systems, Abington, UK)). The mice were kept under normal conditions and one week later sacrificed, and the Matrigel plugs were excised and fixed in 4% paraformaldehyde. The plugs were embedded in paraffin, sectioned and stained with Masson-Trichrome (Sigma-Aldrich) for morphologic evaluation.

Micro-array analysis

To detect down-stream genes and pathways dysregulated in endothelial cells after genetic modulation of MEF2 signaling as well as to assess potential overlap in activity with VEGF, murine Eoma cell cultures were infected at 200 MOI with Ad-empty, Ad-caMEF2, Ad-caMEF2 + VEGF (50 ng/ml) and with Ad-dnMEF2 + VEGF (N=3 per group). After two days, infection efficiency was assessed by the percentage of gated GFP^+ cells via a Fluoresence Activated Cell Sorter (FACSCalibur, BD Biosciences). Cell collections with a minimum of 40% GFP positivity

were used. Afterwards, total RNA was isolated from infected cells according to Chomczynski and Sacchi and cRNA was generated as previously described [15,16]. Equal amounts of cRNA from three pooled RNA samples per condition were hybridized to ABI Mouse Genome Survey Arrays (Applied Biosystems, Foster City, CA) according to the manufacturer's instructions and the arrays were performed and analyzed as previously described [16]. Genes were considered significantly dysregulated as their log fold change (as compared to the Ad-empty group) was greater than the average ± 2-times the standard deviation fold change of all genes measured. Differentially regulated genetic pathways were identified by the Protein ANalysis THrough Evolutionary Relationships (PANTHER) classification system (www.pantherdb.org) [17].

Validation of gene expression by real-time PCR.

cDNA was generated for all microarray samples (N=3 per group) with RevertAid M-MuLV reverse transcriptase (Fermentas, Burlington, Canada) according to manufacturer's protocol. Semi-quantitative gene expression analysis was performed on a selection of genes which constituted significantly regulated pathways as determined by PANTHER using the SYBR-Green method on a Taqman apparatus (Applied Biosystems) with primers, designed using Primer 3 (version 0.4.0) software [18], depicted in table 1. Relative expression was calculated as described previously [19], with hypoxanthine phosphoribosyltransferase (HPRT) as housekeeping gene.

Statistics

All values are expressed as mean ± SEM. Two groups with a single outcome were compared with Student's t-test or Mann-Whitney test when appropriate. One-way ANOVA was used to test single outcomes in three groups with Tuckey's analysis between groups. Two-way ANOVA was used to compare two outcomes between three groups. A P-value of <0.05 was considered significant.

Table 1. Primer sequences used for RT-PCR analysis.

Gene	Forward	Reverse
Actr-β1	AAAATCAAGATCTCTGCTCCTCA	TTCCTTTTTGGATACCCACATC
Ang2	AGATGTCAACACCTTTATCCATGAC	CTTGCTTATTCTTAAATTTCGTCCA
Gsk3β	AGAGAAATGAACCCAAATTATACAGAA	AAGACCTTTGTCCAAGGATGTG
Ptpn1	AGCATGAGTCCAGACACTGAAG	GACAGACGCCTGAGCACTTT
HDAC4	TAGGCGTCAAACCTGCTGAG	CTTCGGGCTACAGTGGTGGT
HDAC5	GACTTGACCGCCATCTGTGA	CATTGACGCTGGGCTTTTG
HPRT	TTGCTCGAGATGTCATGAAGGA	AGCAGGTCAGCAAAGAACTTATAG

RESULTS

Ad-dnMEF2 induces phenotypic changes in plaques

The infected atherosclerotic plaques showed overt expression of GFP, indicating that the adenoviral gene transfer was effective (figure 1A-D). Two weeks of MEF2 activity disruption or

activation induced no significant differences in plaque morphometry (data not shown). Furthermore, no differences were observed in the percentage of luminal stenosis as well as necrotic cores (data not shown). Regarding plaque composition, we compared macrophage presence not only within the three treatment groups, but also between adenovirus incubated and non-incubated contralateral left carotid arteries. These studies revealed that macrophage content was comparable between the three treated and non-treated groups (figure 1E), although a general but minor increase in macrophage presence was noted upon adenoviral infection. However, the sub-group comparative analysis between both carotids from the same mouse showed an enhanced macrophage presence only within Ad-dnMEF2 treated groups (P<0.001), which therefore is indirectly indicative of enhanced macrophage presence. Furthermore, we observed a slight tendency towards increased VSMC presence in Ad-caMEF2 infected plaques as

Figure 1.

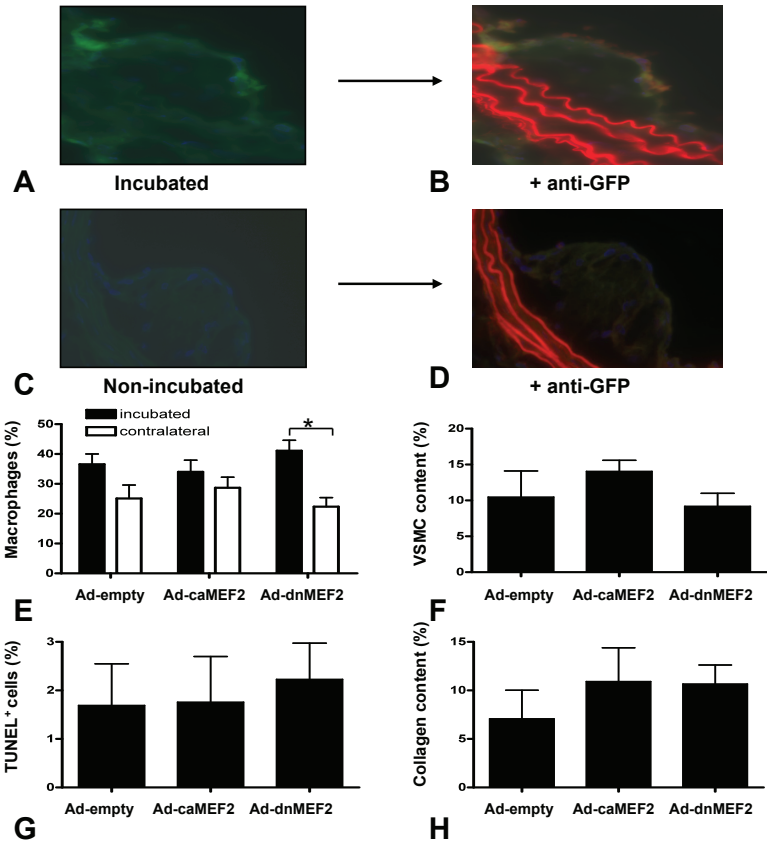

Adenoviral infection after the local in situ incubation of the atherosclerotic vessel segment was successful as judged by GFP positive cells and staining for GFP presence (A,B), whereas in contralateral non-incubated arteries GFP positive cells could not be detected (C,D). No differences in macrophage staining were observed between groups in incubated and sham operated arteries (E). However, comparison of incubated and sham operated arteries in the Ad-dnMEF2 group revealed an enhanced macrophage presence in the former (E). VSMC content showed a non-significant tendency to increase in Ad-caMEF2 incubated arteries (F). No differences were observed between groups in apoptotic cells as assessed by TUNEL staining and in collagen content (G,H). Values are expressed as mean ± SEM, * P<0.001. For color figure see page: 229

Figure 2.

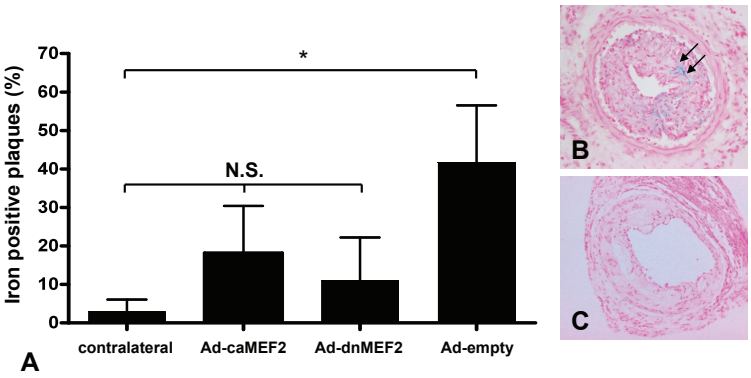

Analyses of iron, indicating haemoglobin presence, within the plaques revealed an increased rate of plaque bleeding in Ad-dnMEF2 but not in Ad-caMEF2 and Ad-empty treated arteries (P=0.24, A). Compared with contralateral sham operated arteries, a significant difference was indeed present. Panels B and C show representative pictures of Ad-dnMEF2 and Ad-empty infected arteries respectively. Values are expressed as mean ± SEM, arrows indicate intraplaque haemorrhages, * P<0.01. For color figure see page: 230

well, albeit not significant (P=0.29, figure 1F). Viral incubation did neither affect apoptotic rates nor collagen content (figure 1G,H). Finally, we made the striking observation that Ad-dnMEF2 infected plaques had much more intra-plaque haemorrhages compared to non-infected, sham operated contralateral arteries as assessed by the presence of iron within the plaque (P<0.01, figure 2). Ad-dnMEF2 showed a non-significant tendency towards more iron positivity within the plaques compared to Ad-empty, suggestive of intraplaque haemorrhage prior to sacrifice. The localization of MEF2A protein in human endothelial cells and our discovery of increased intraplaque haemorrhage prompted us to study the effects of MEF2 activity modulation on endothelial cells by immunohistochemical analysis of CD31 [2]. This revealed a normal $CD31^+$ staining pattern in Ad-caMEF2 and Ad-empty treated plaques, whereas the percentage of $CD31^+$ cells in caps of Ad-dnMEF2 infected plaques was sharply reduced (figure 3A-C). Appar-

Figure 3.

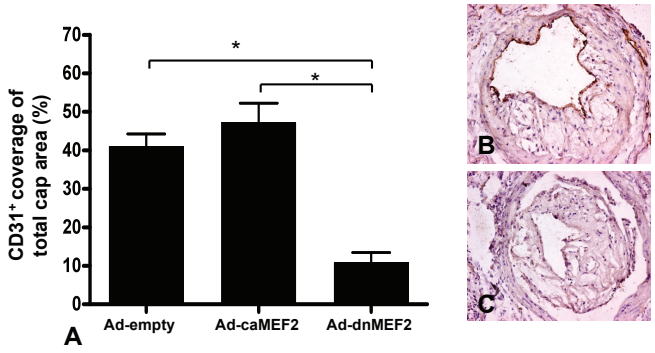

$CD31^+$ coverage, representing endothelial lining, was markedly diminished in Ad-dnMEF2 infected carotid arteries (A). Overt $CD31^+$ staining was seen in Ad-caMEF2 infected arteries, but not in Ad-dnMEF2 infected arteries (B,C). Values are expressed as mean ± SEM, * P<0.001. For color figure see page: 230

ently, blunting of MEF2 transcription promotes endothelial cell desquamation in vivo, leading to plaque erosion and enhanced bleeding within the plaque.

Cellular responses to MEF2 activity modulation

To map the effects of MEF2 activity observed on endothelial cells *in vivo*, we performed *in vitro* Matrigel and proliferation assays after infection of cells with Ad-caMEF2, Ad-dnMEF2 and Ad-empty at a non-cytotoxic virus titer of 100 MOI. Ad-caMEF2 infected HUVECs showed the same amount of cellular junctions in Matrigel coated wells compared to Ad-empty infected cells, however Ad-dnMEF2 infected cells were more scattered and largely devoid of cellular junctions ($P<0.0001$, figure 4A,D-F). Moreover, Ad-dnMEF2 infected HUVECs formed significantly less cellular filipodia as assessed by the total distance of cumulative filipodia length per field ($P=0.001$, figure 4B,D-F). Finally, Ad-caMEF2 infected HUVECs showed enhanced proliferative growth, as the total well area covered by cells was significantly increased compared with Ad-empty infected cells ($P=0.01$, figure 4C). The latter observation is in agreement with the proliferation assay data, as Ad-caMEF2 treated H5V cells displayed a 3-fold increase in [^{3}H] thymidine

Figure 4.

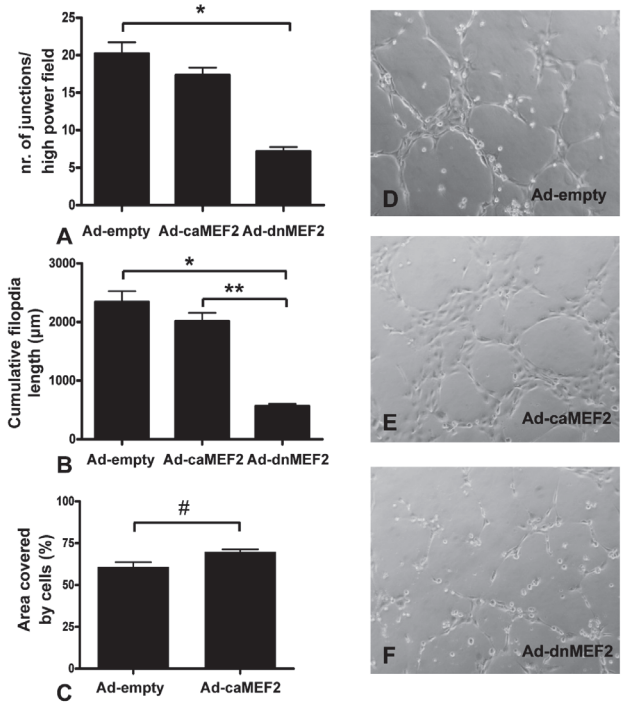

Ad-dnMEF2 infected HUVECs showed less cellular junctions with a decreased total length of interconnecting filopodia on a Matrigel matrix (A,B). Ad-caMEF2 enhanced cellular growth, as assessed by a 15% relative increase in percentage of the area covered by cells (C). Representative pictures of the three different groups (D-F). Values are expressed as mean ± SEM, * $P<0.01$, ** $P<0.05$ and # $P=0.01$

incorporation (P=0.015, supplemental figure 1). Therefore, abrogation of MEF2 signaling *in vitro* leads to decreased endothelial cell function, whereas amplifying MEF2 activity enhances the endothelial proliferative response.

Matrigel *in vivo* analysis

We used the *in vivo* plug assay based on Ad-caMEF2, Ad-dnMEF2 and Ad-empty containing Matrigel to support our Matrigel MEF2 *in vitro* observations in a more physiological environment. Cellular GFP presence was apparent in the plugs, establishing effective viral infection during ingrowth (figure 5A). Without the addition of VEGF to the Matrigel plugs, we observed diminished cellular infiltration of cells into the border zone of Ad-dnMEF2 infected Matrigel plugs after 1 week (figure 5B,D,F). Ad-dnMEF2 treated plugs also resulted in distinct morphological changes, evidenced by more rounded cells and less cellular elongation in cells within the plugs compared to Ad-empty and Ad-caMEF2 treated plugs. After addition of VEGF to the Matrigel plugs, no differences in cellular infiltration as well as cellular phenotype were observed in the Ad-empty treated plugs (figure 5C). Interestingly, an enhanced proliferative response

Figure 5.

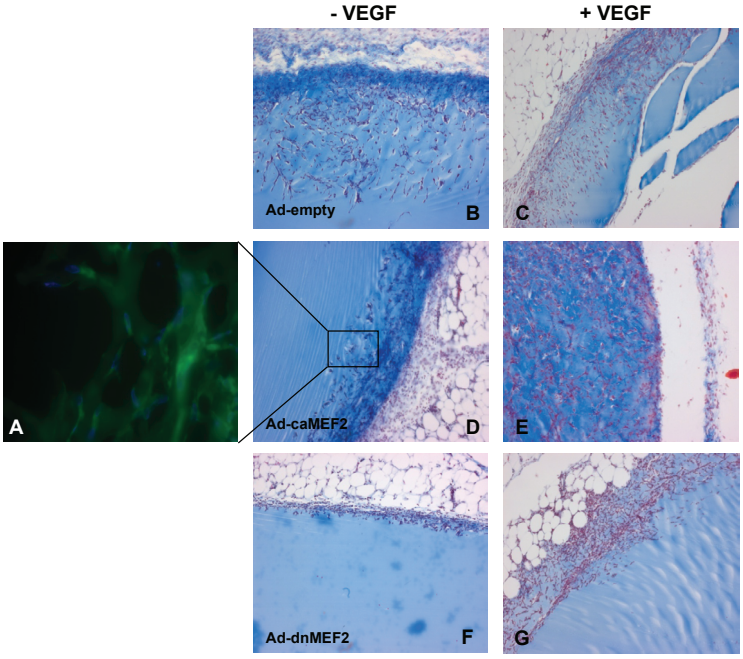

Representative pictures of adenovirus containing Matrigel *in vivo* plugs in C57Bl6 mice. Infiltrated cells within the Matrigel plug were GFP positive, indicating successful adenoviral infection (A). Without VEGF, cellular infiltration into Ad-dnMEF2 treated plugs was markedly diminished compared to Ad-empty plugs (B,D,F). Also, note the stretched cellular phenotype in Ad-empty plugs compared to the more rounded phenotype in Ad-caMEF2 and Ad-dnMEF2 treated plugs. Addition of VEGF did not induce obvious differences in Ad-empty treated plugs; however cellular infiltration was markedly enhanced in Ad-caMEF2 plugs, whereas VEGF marginally enhanced cellular growth in Ad-dnMEF2 plugs. For color figure see page: 231

with an identical cellular morphology compared to the Ad-empty infected group was seen in the Ad-caMEF2 treated plugs, indicating that VEGF amplifies the MEF2 induced proliferative response (figure 5E). A smaller increase in cellular growth was seen in the Ad-dnMEF2 group, showing not only that VEGF partly rescues the changes induced by MEF2 transcriptional abrogation (figure 5G), but also that MEF2 inhibition partly counteracts VEGF activity.

Microarray analysis – Gene expression

Based on these findings, we hypothesized that MEF2 might induce a similar proliferative and angiogenic response as VEGF. To test this as well as to examine endothelium specific downstream targets and pathways of MEF2 signaling, we undertook a microarray analysis of Ad-empty, Ad-empty+VEGF, Ad-caMEF2 and Ad-dnMEF2+VEGF infected HUVECs. We observed expression of 11,150 genes in the Ad-empty infected control endothelial cells. In Ad-empty treated cells, co-incubated with VEGF, 695 genes were differentially regulated (> ± 2-times SD) compared with Ad-empty infected cells. Ad-caMEF2 infection resulted in 545 differentially regulated genes, whereas Ad-dnMEF2 infection with VEGF versus Ad-empty with VEGF caused a differential regulation of 548 genes. Of interest, analysis of Ad-dnMEF2 with VEGF versus Ad-empty yielded less regulated genes. Comparative analysis of the overlap between Ad-caMEF2 infection and VEGF incubation revealed a remarkably high number of 199 identically regulated genes, with 194 up- and 5 down-regulated overlapping genes in both groups, as compared to only 2 genes which were down-regulated by VEGF but up-regulated by Ad-caMEF2.

Microarray – Pathway analysis

Genes that were differentially expressed on the microarray chips were subsequently analysed with the PANTHER algorithm, based on a database of genes classified into families and subfamilies of shared function, which categorizes genes by molecular function, biological process and pathway. The transcriptome of the Ad-empty infected group was used as the reference gene list for differentially regulated genes in the 3 treatment groups. Furthermore, we mainly focussed on the classification of genetic pathways rather than individual genes. Comparative analysis with Ad-caMEF2 infected cells revealed 5 significantly up-regulated pathways ($P<0.05$, table 2), with the Cadherin and Wnt signaling pathway showing highest significance. These observations suggest that MEF2 is a transcriptional activator of Cadherin related genes and via this route controls the angiogenic response. Incubation of mouse endothelial cells with VEGF resulted in an up-regulation of 7 pathways, including the Insulin/IGF pathway-protein kinase B and the Cadherin signaling pathways (table 1B). The comparative analysis of Ad-dnMEF2/VEGF with Ad-empty/VEGF revealed but one signaling pathway to be significantly up-regulated, notably the Insulin/IGF pathway-protein kinase B, suggesting that the regulation of this VEGF sensitive pathway may be MEF2 dependent. However, the Insulin/IGF pathway-protein kinase B mainly comprised a different selection of Forkhead transcription factors as seen in the Ad-empty+VEGF treated group. FoxO1 and FoxC1 were down-regulated, whereas the other genes were up-regulated (table 3), suggesting that MEF2 and VEGF act in a largely overlapping but

Table 2. Overview of significantly regulated PANTHER pathways.

Ad-caMEF2 versus Ad-empty				
Pathways	Total pickup (reference)	Observed genes	Ratio of enrichement	P-value
Cadherin signaling pathway	54	10	3.78	0.0004
Wnt signaling pathway	145	13	1.83	0.028
Cytoskeletal regulation by Rho GTPase	60	7	2.39	0.030
FAS signaling pathway	26	4	3.15	0.040
Leucine biosynthesis	1	1	20	0.047
Ad-empty+VEGF versus Ad-empty				
Pathways	Total pickup (reference)	Observed genes	Ratio of enrichement	P-value
Insulin/IGF pathway-protein kinase B signaling cascade	40	8	3.21	0.004
Cadherin signaling pathway	54	9	2.67	0.008
PI3 kinase pathway	59	9	2.44	0.013
Pentose phosphate pathway	8	3	6	0.014
Interleukin signaling pathway	81	11	2.18	0.014
EGF receptor signaling pathway	80	10	2	0.031
Endothelin signaling pathway	50	7	2.24	0.039
Ad-dnMEF2+VEGF versus Ad-empty+VEGF				
Pathways	Total pickup (reference)	Observed genes	Ratio of enrichement	P-value
Insulin/IGF pathway-protein kinase B signaling cascade	40	6	3.04	0.015
Ad-dnMEF2+VEGF versus Ad-empty				
Pathways	Total pickup (reference)	Observed genes	Ratio of enrichement	P-value
Insulin/IGF pathway-protein kinase B signaling cascade	40	6	3.63	0.006
TGF-beta signaling pathway	67	8	2.90	0.007
PI3 kinase pathway	59	6	2.47	0.037
overlap Ad-caMEF2 versus Ad-empty+VEGF				
Pathways	Total pickup (reference)	Observed genes	Ratio of enrichement	P-value
Cadherin signaling pathway	54	6	6.18	0.0005
Axon guidance mediated by Slit/Robo	11	2	10	0.017
Leucine biosynthesis	1	1	50	0.018
Cytoskeletal regulation by Rho GTPase	60	4	3.70	0.024
Valine biosynthesis	2	1	25	0.035
Insulin/IGF pathway-protein kinase B signaling cascade	40	3	4.16	0.036
Unclassified	9836	169	0.95	0.048

not essentially identical manners. The remaining 6 pathways which were dysregulated in the separate Ad-empty+VEGF analysis were no longer observed, suggesting an exclusive MEF2 dependent activation of these pathways. No down-regulated pathways were observed, which suggests that MEF2 activates pathways in concert with VEGF. In line with these findings, the

TGF-β signaling and PI3 kinase pathway were additionally up-regulated in Ad-dnMEF2+VEGF treated cells as compared to Ad-empty treated cells in comparison with the previous analysis, which is therefore solely regulated by VEGF activity.

Next, we compared the expression profiles of Ad-caMEF2 and VEGF to assess the overlap of regulated genes and pathways. This showed an overlapping expression of 6 up-regulated pathways and 1 down-regulated unclassified pathway (table 2). The Cadherin pathway was, once again, highly regulated, supporting the notion that MEF2 has overlapping functionality and/or acts in concert with VEGF, which might explain the pro-angiogenic features of Ad-caMEF2 seen on endothelial cells *in vitro*.

HDAC-MEF2 interaction in endothelial cells

MEF2 activity was seen to be regulated at a transcriptional level by, among others, Histone Deacetylases (HDACs) [3]. MEF2 dependent changes in expression of class II HDAC4 and 5 were

Figure 6.

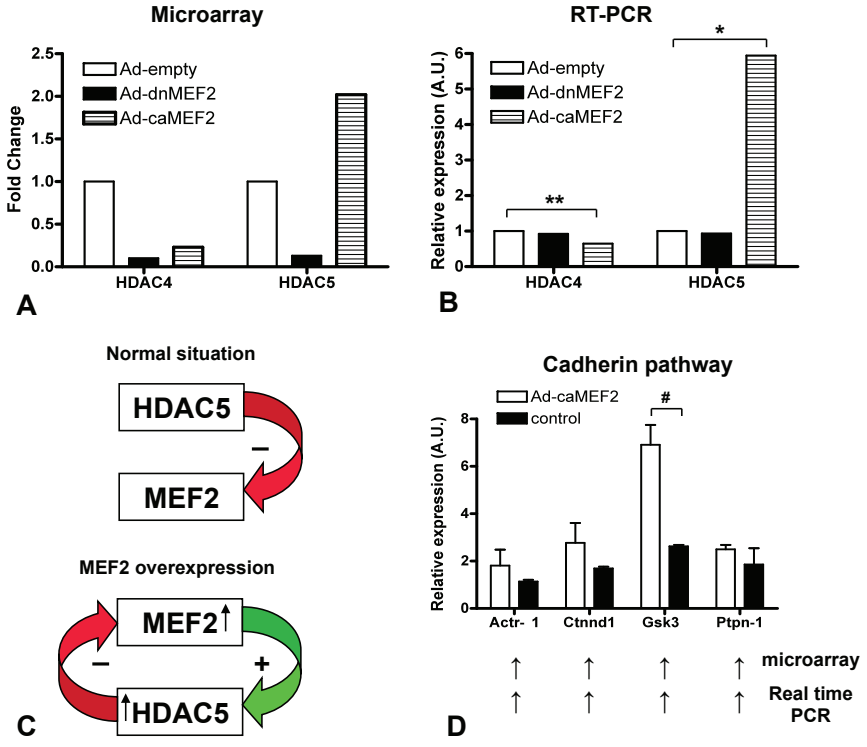

HDAC expression in Ad-caMEF2, Ad-dnMEF2 and Ad-empty infected cells as detected by microarray and verified with RT-PCR. Expression patterns differences observed with microarray were less prominent by RT-PCR analysis, except for HDAC5 which showed a significant 6-fold increase in Ad-caMEF2 treated cells (A,B) MEF2 overexpression might therefore induce a negative feedback loop with HDAC5 (C). RT-PCR verification analysis of the Cadherin signaling pathway. Genes were similarly affected as observed with the micro-array, but only Gsk3β reached significance, ↑ = expression up-regulated (D). Values are expressed as mean ± SEM, * P=0.02, ** P<0.001 and # P<0.01

observed in the microarray and verified with RT-PCR (figure 6A,B). Both HDAC4 and 5 were down-regulated by Ad-dnMEF2, while HDAC4 was down-regulated by Ad-dnMEF2 but up-regulated by Ad-caMEF2, possibly reflective of a feedback loop between MEF2 and HDAC4 and 5 activity in endothelial cells blunting elevated MEF2 activities (figure 6C).

Microarray real time-PCR verification analysis

A selection of genes constituting the Cadherin signaling as well as the Insulin/IGF pathway-protein kinase B signaling pathway were selected for additional real time-PCR verification analysis. Regarding the Cadherin signaling pathway, all four tested genes showed the identical up-regulated pattern as the microarray, but only expression of Gsk3β was significantly altered ($P<0.01$, figure 6D). Five genes in the Insulin/IGF pathway-protein kinase B signaling pathway showed the same pattern as the microarray (data not shown).

DISCUSSION

This study shows that 1) MEF2 activity leads to decreased endothelial cell viability *in vivo,* 2) MEF2 is critical for proper endothelial cell function *in vitro* and 3) MEF2 regulates genetic pathways, similar to VEGF, involved in endothelial cell homeostasis.

In their genetic linkage analysis, Wang et al. identified a deletion of 7 amino acids which resulted in diminished MEF2 function in HUVECs as well as human VSMCs *in vitro* [2]. We assessed if modulation of MEF2 activity would also lead to alterations in endothelial and atherosclerotic plaque phenotype *in vivo*. Using a locally applied viral vector delivery strategy in ApoE-/- mice, we were able to alter MEF2 function solely at the area of interest, the advanced atherosclerotic plaque. No significant differences were observed on plaque size and morphology upon MEF2 activation or repression. This suggests that local MEF2 activity modulation does not induce phenotypic changes, or the 2-week period of MEF2 overexpression was too short to exert any effect.

As MEF2 proteins are expressed in endothelial during development [6], previous reports already have shown the critical dependence of MEF2 activity for proper endothelial cell function, which is suggested to be mainly mediated by MEF2A and MEF2C [9]. The endothelium is an essential cell boundary between blood and the atherosclerotic plaque. Malfunctioning endothelium will be more prone to inflammation and the formation and destabilization of an atherosclerotic plaque which may result in thrombosis, myocardial infarction, and sudden death. We observed a remarkable decrease in $CD31^+$ staining when MEF2 was abrogated, which indicated that the endothelial layer was less viable or even absent. This could also explain the enhanced tendency of iron presence within the plaques, which might be caused by leakage through the endothelial layer of the vascular lumen or via influx through intra-plaque capillaries. Furthermore, as we gained indirect evidence of enhanced macrophage presence arteries expressing decreased MEF2 activity, defective or loss of endothelial cells might enhance infiltration of macrophages and other cell-types into the plaque, enhancing a rupture prone phenotype.

The effects of MEF2 activity modulation were additionally assessed *in vitro*, where enhanced MEF2 activation not only induced marked proliferation of endothelial cells, but MEF2 activity modulation also markedly influenced HUVEC function in a 2-dimensional Matrigel matrix. Cellular networks were nearly absent in cells with decreased MEF2 activity and were not capable of forming proper cell-cell contact, showing that MEF2 function is highly critical for endothelial cell homeostasis. Moreover, Ad-dnMEF2 Matrigel *in vivo* analysis induced a diminished infiltrative cellular growth of cells as well as less stretching of the cells which points to a severely disorganised 3-dimensional cell-cell interaction. These phenotypic changes were however also partly seen in the Ad-caMEF2 treated plugs, indicating that MEF2 overexpression does not trigger an enhanced neo-angiogenic response and leads to hampered cellular proliferation *in vivo*. Addition of VEGF to the Matrigel plugs resulted in a strong infiltrative cellular response in the Ad-caMEF2 and to a lesser extent in the Ad-dnMEF2 groups, amplifying the effects of MEF2 activation and rescuing the adverse effects of MEF2 abrogation. Of interest, the dramatic effects of diminished MEF2 signaling are in concordance with the observations Hayashi et al., as they demonstrated that conditional deletion of ERK5, a key MEF2 regulator, resulted in round, irregularly aligned and apoptotic endothelial cells lining blood vessels [8]. The downstream genetic targets of ERK5-MEF2 signaling in endothelial cells have thus far not been elucidated, but may constitute a similar pattern as those regulated by VEGF, as this growth factor activates ERK5 [9]. In our microarray, performed to study these questions, we detected enhanced expression of a number of genes and pathways critically involved endothelial cell function, like the Cadherin pathway which was regulated both in the Ad-caMEF2 and in the VEGF stimulated cells. Verification analysis showed a significant increase of glycogen synthase kinase (Gsk)3β, which has a crucial function in endothelial cell homeostasis and regulates angiogenesis [20]. Furthermore, the Insulin/IGF pathway-protein kinase B signaling cascade, constituting various Forkhead box transcription factors, was also induced by both VEGF and MEF2 activation. VEGF-forkhead signaling, through a PI3K/Akt-dependent pathway, is a regulator of endothelial cell function [21], but forkhead signaling has not yet been linked to MEF2 regulation in endothelial cells. Various Forkhead box transcription factors like FoxO1, which is highly down-regulated upon MEF2 disruption, are seen to act as critical regulators controlling endothelial proliferation and survival [22]. MEF2 is likely to exert its influence on endothelial cells partly via this way. Altogether, these associations strongly suggest that MEF2 and VEGF might act through a similar signaling cascade, thereby regulating similar sets of downstream target genes. In addition, comparison of MEF2 activity disruption with the effects of VEGF showed that only the Insulin/IGF pathway-protein kinase B signaling cascade was differentially regulated, although via other Forkhead box transcription factors. MEF2 repression markedly decreased expression of FoxO1, which might be due to a negative feedback loop in response to the dramatic phenotype of Ad-dnMEF2 infected endothelial cells, as silencing of FoxO1 led to a clear increase in migratory capacities of endothelial cells [22]. Therefore, MEF2 repression regulates other Forkhead box transcription factors than the ones that are activated by the VEGF signaling cascade, which shows that MEF2 signaling in endothelial cells does not follow the exact same pathways as

VEGF signaling. Finally, modulation of MEF2 activity also has an effect on regulators of MEF2 function itself, like HDAC4 and HDAC5. Under physiological conditions, MEF2 transcriptional activity is repressed by HDAC4 and HDAC5 [23]. Although a regulatory feedback mechanism had been shown for other HDAC isoforms like HDAC9 [24], we show that general MEF2 overexpression induces a feedback loop to HDAC expression, as we observed a strong increased expression of HDAC5 and a moderately decreased expression of HDAC4. This might suggest that HDAC5 is more responsive for MEF2 modulation, but this notion, together with its functional implication, has to be studied in more detail.

In conclusion, MEF2 inactivation significantly suppressed neo-intima formation in wire injury model of rat femoral arteries [4]. Given the phenotypic changes seen on endothelial cells and plaques, we are the first to extend this neo-intimal anti-proliferative observation in a model of advanced atherosclerosis, leading to enhanced plaque haemorrhage. Furthermore, there is currently some debate whether or not MEF2(A) indeed clinically plays a significant role. The results by Wang et al., who have claimed that 1.93% of all CAD patients may carry a mutation in the MEF2A gene [25], are supported by two other reports which linked single nucleotide polymorphisms in the MEF2A gene to CAD but are challenged by other papers, including a recently published large population study, stating that mutations in the MEF2A gene do not cause autosomal dominant forms of CAD [26-29]. We provide direct experimental evidence that causally links diminished MEF2 transcriptional activity with endothelial dysfunction and plaque erosion in vivo. Therefore, we not only believe that certain MEF2A polymorphisms indeed seem to be a significant causal factor in CAD but that MEF2, or downstream targets thereof, may constitute an attractive target in the prevention of plaque erosion.

Acknowledgements

We would like to thank Peter van Santbrink for technical assistance.

REFERENCES

1. Miller DT, Ridker PM, Libby P, Kwiatkowski DJ. Atherosclerosis: the path from genomics to therapeutics. *J Am Coll Cardiol*. 2007;49:1589-99.
2. Wang L, Fan C, Topol SE, Topol EJ, Wang Q. Mutation of MEF2A in an inherited disorder with features of coronary artery disease. *Science*. 2003;302:1578-81.
3. Potthoff MJ, Olson EN. MEF2: a central regulator of diverse developmental programs. *Development*. 2007;134:4131-40.
4. Suzuki E, Satonaka H, Nishimatsu H, Oba S, Takeda R, Omata M, Fujita T, Nagai R, Hirata Y. Myocyte enhancer factor 2 mediates vascular inflammation via the p38-dependent pathway. *Circ Res*. 2004;95:42-9.
5. Naya FJ, Black BL, Wu H, Bassel-Duby R, Richardson JA, Hill JA, Olson EN. Mitochondrial deficiency and cardiac sudden death in mice lacking the MEF2A transcription factor. *Nat Med*. 2002;8:1303-9.
6. Lin Q, Lu J, Yanagisawa H, Webb R, Lyons GE, Richardson JA, Olson EN. Requirement of the MADS-box transcription factor MEF2C for vascular development. *Development*. 1998;125:4565-74.
7. Firulli AB, Miano JM, Bi W, Johnson AD, Casscells W, Olson EN, Schwarz JJ. Myocyte enhancer binding factor-2 expression and activity in vascular smooth muscle cells. Association with the activated phenotype. *Circ Res*. 1996;78:196-204.
8. Hayashi M, Kim SW, Imanaka-Yoshida K, Yoshida T, Abel ED, Eliceiri B, Yang Y, Ulevitch RJ, Lee JD. Targeted deletion of BMK1/ERK5 in adult mice perturbs vascular integrity and leads to endothelial failure. *J Clin Invest*. 2004;113:1138-48.
9. Olson EN. Undermining the endothelium by ablation of MAPK-MEF2 signaling. *J Clin Invest*. 2004;113:1110-2.
10. van Oort RJ, van Rooij E, Bourajjaj M, Schimmel J, Jansen MA, van der Nagel R, Doevendans PA, Schneider MD, van Echteld CJ, De Windt LJ. MEF2 activates a genetic program promoting chamber dilation and contractile dysfunction in calcineurin-induced heart failure. *Circulation*. 2006;114:298-308.
11. He TC, Zhou S, da Costa LT, Yu J, Kinzler KW, Vogelstein B. A simplified system for generating recombinant adenoviruses. *Proc Natl Acad Sci U S A*. 1998;95:2509-14.
12. von der Thusen JH, van Berkel TJ, Biessen EA. Induction of rapid atherogenesis by perivascular carotid collar placement in apolipoprotein E-deficient and low-density lipoprotein receptor-deficient mice. *Circulation*. 2001;103:1164-70.
13. von der Thusen JH, van Vlijmen BJ, Hoeben RC, Kockx MM, Havekes LM, van Berkel TJ, Biessen EA. Induction of atherosclerotic plaque rupture in apolipoprotein E-/- mice after adenovirus-mediated transfer of p53. *Circulation*. 2002;105:2064-70.
14. de Nooijer R, Verkleij CJ, von der Thusen JH, Jukema JW, van der Wall EE, van Berkel TJ, Baker AH, Biessen EA. Lesional overexpression of matrix metalloproteinase-9 promotes intraplaque hemorrhage in advanced lesions but not at earlier stages of atherogenesis. *Arterioscler Thromb Vasc Biol*. 2006;26:340-6.
15. Chomczynski P, Sacchi N. Single-step method of RNA isolation by acid guanidinium thiocyanate-phenol-chloroform extraction. *Anal Biochem*. 1987;162:156-9.
16. Hoekstra M, Stitzinger M, van Wanrooij EJ, Michon IN, Kruijt JK, Kamphorst J, Van Eck M, Vreugdenhil E, Van Berkel TJ, Kuiper J. Microarray analysis indicates an important role for FABP5 and putative novel FABPs on a Western-type diet. *J Lipid Res*. 2006;47:2198-207.
17. Thomas PD, Kejariwal A, Guo N, Mi H, Campbell MJ, Muruganujan A, Lazareva-Ulitsky B. Applications for protein sequence-function evolution data: mRNA/protein expression analysis and coding SNP scoring tools. *Nucleic Acids Res*. 2006;34:W645-50.
18. Rozen S, Skaletsky H. Primer3 on the WWW for general users and for biologist programmers. *Methods Mol Biol*. 2000;132:365-86.
19. t Hoen PA, Van der Lans CA, Van Eck M, Bijsterbosch MK, Van Berkel TJ, Twisk J. Aorta of ApoE-deficient mice responds to atherogenic stimuli by a prelesional increase and subsequent decrease in the expression of antioxidant enzymes. *Circ Res*. 2003;93:262-9.
20. Skurk C, Maatz H, Rocnik E, Bialik A, Force T, Walsh K. Glycogen-Synthase Kinase3beta/beta-catenin axis promotes angiogenesis through activation of vascular endothelial growth factor signaling in endothelial cells. *Circ Res*. 2005;96:308-18.
21. Abid MR, Shih SC, Otu HH, Spokes KC, Okada Y, Curiel DT, Minami T, Aird WC. A novel class of vascular endothelial growth factor-responsive genes that require forkhead activity for expression. *J Biol Chem*. 2006;281:35544-53.
22. Potente M, Urbich C, Sasaki K, Hofmann WK, Heeschen C, Aicher A, Kollipara R, DePinho RA, Zeiher AM, Dimmeler S. Involvement of Foxo transcription factors in angiogenesis and postnatal neovascularization. *J Clin Invest*. 2005;115:2382-92.
23. Lu J, McKinsey TA, Nicol RL, Olson EN. Signal-dependent activation of the MEF2 transcription factor by dissociation from histone deacetylases. *Proc Natl Acad Sci U S A*. 2000;97:4070-5.
24. Haberland M, Arnold MA, McAnally J, Phan D, Kim Y, Olson EN. Regulation of HDAC9 gene expression by MEF2 establishes a negative-feedback loop in the transcriptional circuitry of muscle differentiation. *Mol Cell Biol*. 2007;27:518-25.
25. Bhagavatula MR, Fan C, Shen GQ, Cassano J, Plow EF, Topol EJ, Wang Q. Transcription factor MEF2A mutations in patients with coronary artery disease. *Hum Mol Genet*. 2004;13:3181-8.

26. Gonzalez P, Garcia-Castro M, Reguero JR, Batalla A, Ordonez AG, Palop RL, Lozano I, Montes M, Alvarez V, Coto E. The Pro279Leu variant in the transcription factor MEF2A is associated with myocardial infarction. *J Med Genet*. 2006;43:167-9.
27. Han Y, Yang Y, Zhang X, Yan C, Xi S, Kang J. Relationship of the CAG repeat polymorphism of the MEF2A gene and coronary artery disease in a Chinese population. *Clin Chem Lab Med*. 2007;45:987-92.
28. Weng L, Kavaslar N, Ustaszewska A, Doelle H, Schackwitz W, Hebert S, Cohen JC, McPherson R, Pennacchio LA. Lack of MEF2A mutations in coronary artery disease. *J Clin Invest*. 2005;115:1016-20.
29. Lieb W, Mayer B, Konig IR, Borwitzky I, Gotz A, Kain S, Hengstenberg C, Linsel-Nitschke P, Fischer M, Doring A, Wichmann HE, Meitinger T, Kreutz R, Ziegler A, Schunkert H, Erdmann J. Lack of association between the MEF2A gene and myocardial infarction. *Circulation*. 2008;117:185-91.